XXV CONGRESO NACIONAL DE INGENIERÍA MECÁNICA
Santander, 10-13 junio 2025
UC Universidad de Cantabria
IFToMM

Modeling, Analysis, and Actuator Selection of a Wing Folding and Unfolding Device for an Urban Air Mobility Vehicle

Carlos Pérez-Carrera[1], Carmine Maria Pappalardo[1], Domenico Guida[1], Higinio Rubio[2]

[1] *Department of Industrial Engineering, University of Salerno (Italy), cperezcarrera@unisa.it, cpappalardo@unisa.it, guida@unisa.it*

[2] *Department of Mechanical Engineering, University Carlos III of Madrid, hrubio@ing.uc3m.es*

In the context of urban air mobility, personal flying vehicles represent an emerging solution to congestion problems in densely populated urban areas and a potential means of reducing travel times. Such vehicles necessitate the integration of sophisticated mechanical systems to facilitate a seamless transition between ground and air modes. One of the fundamental challenges is the development of an effective and reliable wing folding and deployment mechanism. This study commences with the multibody modeling of a wing folding and unfolding system for a flying car. Such modeling will facilitate an accurate representation of the dynamic behavior of complex mechanical systems, which is essential for the evaluation and optimization of critical components of the mechanical device. The primary objective of this study is to ascertain the requisite force generated by the electric piston to facilitate the folding and unfolding of the wings, given that they support the engines and propellers that are responsible for lift and control during flight. This information will facilitate the selection of an appropriate electric actuator, capable of performing the required action in an efficient and safe manner. The analysis will consider the inertia forces and the weight of the components at the moment of folding or unfolding. A second objective of this study is to calculate the reactions acting on the electric actuator when the vehicle is in flight, under conditions that may be considered unfavorable. These conditions will represent extreme scenarios in which structural stability of the mechanism is of paramount importance, as inadvertent closure of the wings during flight could result in catastrophic consequences. To address the aforementioned aspect, the forces and moments that the actuator must withstand to maintain wing deployment will be analyzed. Furthermore, the mechanism's stability under these loading conditions will be tested. The device's modeling will facilitate the simulation of diverse operational scenarios and the evaluation of the electric actuator's performance requirements, thereby guaranteeing the secure and dependable operation of the wing mechanism. The findings of this analysis will furnish indispensable data for the selection of components and the final design of the folding and unfolding system, thereby contributing to the advancement of solutions for safer and more efficient urban aerial mobility. It seems reasonable to suggest that this methodology could be applied to other flying vehicle projects where safety and efficiency are of paramount importance in the design of flight-to-ground mode transition systems.

1. Introduction

Urban Air Mobility (UAM) represents a transformative vision for modern transportation, addressing the twin issues of growing urban congestion and the need for sustainable mobility solutions. UAM employs advancements in vertical take-off and landing (VTOL) vehicles, autonomous systems, and lightweight structures to facilitate efficient point-to-point travel in urban and peri-urban settings [1, 2]. Among these innovations, flying cars represent a particularly disruptive concept, combining the capabilities of traditional ground vehicles with aerial performance [3].

The integration of folding mechanisms for propulsive arms represents a significant engineering challenge in this domain, as it must ensure the compact design of vehicles for road travel while also guaranteeing operational reliability during flight [4]. The folding arm mechanism represents a vital subsystem in the design of flying cars intended for use with UAM. The mechanism's function is to facilitate the transition of the vehicle between a compact configuration, optimized for terrestrial mobility, and a fully deployed state, which is necessary for flight operations. This dual-purpose functionality imposes rigorous requirements on the design, including elevated mechanical reliability, lightweight composition, and precise control [5]. Among the essential elements of the folding mechanism, the actuator plays an indispensable role in attaining the necessary motion and maintaining structural integrity under diverse loading circumstances [6].

The selection of an efficacious actuator hinges upon a comprehensive grasp of the forces at play during folding, deployment, and flight operations. The latest research on VTOL and flying car systems has identified a growing emphasis on the development of efficient and robust actuator designs. In recent years, studies by Hu et al. [7] and Wang and Dowell [8] have contributed to our understanding of the dynamic behavior of folding wing and arm mechanisms in a range of flight conditions. These investigations underscore the significance of accurately modeling the kinematics and dynamics of the folding process, as well as comprehending the aerodynamic forces acting on the system during flight. Notwithstanding considerable progress in this field, a lacuna persists in the systematic examination of the combined static and dynamic forces exerted on the folding mechanisms, especially in circumstances distinctive to UAM vehicles. In light of these challenges, there is a clear need for a detailed multibody model. Multibody dynamics provides a robust framework for simulating the motion and forces in mechanical systems comprising multiple interconnected components [9]. This modeling approach allows for the prediction of both kinematic and dynamic behavior, thereby providing insights into the forces and moments acting on critical elements such as actuators and joints. Moreover, multibody simulations allow for the assessment of diverse operational scenarios, including the impact of actuation time, load distributions, and external aerodynamic forces [10].

This study addresses these gaps by developing a comprehensive multibody model of the folding arm mechanism in a flying car. In contrast to previous studies that have concentrated on either the dynamic folding process or static loadbearing analysis [11, 12, 13, 14], this research integrates both perspectives to provide a comprehensive understanding of actuator performance. This research study has two specific objectives. The first objective is to quantify the force requirements for the actuator during both the folding and deployment phases, with the understanding that these phases occur over varying periods of time. The second objective is to evaluate the static forces acting on the actuator under conditions of adverse flight, with a particular focus on forward flight, during which there are significant aerodynamic loads. The combination of these analyses ensures that an actuator is selected which meets the dual demands of dynamic motion and static load retention.

2. System description

The folding and deployment mechanism described in this study represents a fundamental component of a flying car designed for UAM. The system permits the vehicle to transition between ground and aerial operations in an uninterrupted and seamless manner, through the extension and retraction of its arms. The aforementioned arms are equipped with motors and propellers that are responsible for generating the necessary lift and thrust for a variety of flight conditions. Although the vehicle is equipped with four foldable arms, this analysis focuses on a single arm to simplify the modeling and computational effort, as all arms are designed to operate symmetrically under identical conditions.

The arm under study is comprised of a hinged structural framework with two axially symmetric motors, one mounted at the upper extremity and the other at the lower extremity. The aforementioned motors drive counterrotating propellers, which, in conjunction, provide the vehicle with stability and balance during flight. The arm is folded via an electric actuator that is connected to a pivoting hinge at its base. When deployed, the arm extends outward and locks into position, thereby forming part of the vehicle's aerodynamically efficient quad-arm configuration. The CAD model of the mechanism, depicted in Figure 1, illustrates the structural arrangement highlighting key elements. This mechanism has been designed to meet two distinct requirements: that of compactness and that of reliability. When folded, the arms reduce the vehicle's spatial footprint, thereby facilitating easier maneuverability on the ground. During its flight, the extended arms provide the requisite

leverage to distribute the thrust generated by the motor, while maintaining the necessary structural integrity to withstand the loads imposed by aerodynamic and inertial forces. The structural arm is constructed from lightweight yet robust materials in order to reduce the overall weight of the structure while maintaining the requisite strength. Each motor is an axially symmetric unit constructed from aluminum, optimized for efficient thrust generation while maintaining a low mass.

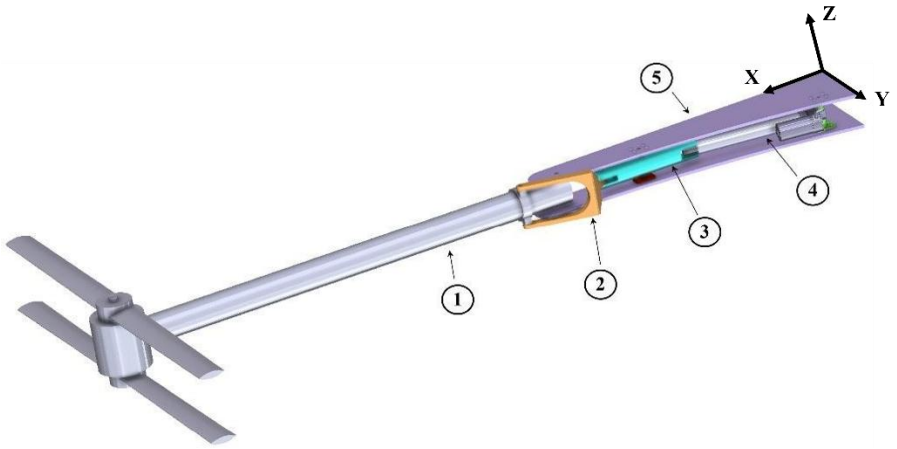

Figure 1: Foldable flying car arm model.

The electric actuator, constructed from a high-strength steel alloy, will be designed to accommodate both the static loads encountered during the folding and deployment phases and the loads experienced during flight. The hinge mechanism is manufactured from Al 2024-T351, an aluminum alloy renowned for its exceptional strength-to-weight ratio and fatigue resistance. A summary of the components and their material specifications is provided in Table 1.

Table 1: Components specifications.

Item	Component	Material
1	Arm system	Composite CFRP
2	Connecting rod	Al 2024-T351
3	Crank	Al 2024-T351
4	Actuator	Al 2024-T351
5	Base	Al 2024-T351

It is imperative that the motors mounted on the arm produce sufficient thrust to lift the entire vehicle during vertical take-off, hovering, and forward flight. The requisite thrust varies depending on the flight condition. Prior studies have indicated that for a 600 kg vehicle, the thrust per motor ranges from 1655.4 N during vertical lift and hover to approximately 3232.1 N during forward flight at a maximum safe inclination angle θ of 45º [15]. Table 2 provides a comprehensive overview of these values, offering a clear representation of the varying operational demands placed on the system.

Table 2: Values of the thrust forces for different values of θ [15].

θ	Force (F_R)
0º	1655.4 N
5º	2468.4 N
15º	2495.7 N
25º	2609.5 N
35º	2835.6 N
45º	3232.1 N

The arm folding mechanism is actuated electrically, thereby ensuring both precision and reliability of operation. During ground operations, the arms are stowed in order to minimize drag and improve maneuverability. Prior to take-off, the actuator deploys the arms into their extended positions, locking them securely in a state of stability,

thus providing a platform suitable for flight. During the course of flight, the extended arms are required to endure aerodynamic forces which vary according to the speed of the vehicle, its inclination angle, as well as environmental conditions, such as wind gusts.

The thrust generated by the motors is critical not only for lift but also for stability and control. In vertical take-off and hover, all thrust is directed upward to counteract gravity and lift the vehicle. In forward flight, the vehicle tilts at an angle to redirect some of the thrust horizontally, enabling forward motion. This tilt reduces the vertical lift component, requiring careful balancing of forces to maintain stable flight. Figure 2 illustrates the thrust distribution during different flight phases, showing the transition from vertical lift to forward flight. In addition to the thrust

requirements, the folding mechanism must handle significant mechanical loads. During deployment, the actuator must overcome the weight of the arm and the motors, as well as any inertial forces arising from the arm's motion. Once deployed, the actuator must remain stable, resisting external forces that could compromise the system's integrity. This is particularly critical during adverse flight conditions, such as strong wind gusts or high- speed maneuvers, where the risk of unintended arm retraction could pose a catastrophic safety hazard. To ensure safe operation, the actuator is designed to meet two key performance criteria. First, it must provide sufficient force to reliably fold and deploy the arm, considering the arm's weight and the forces acting on it during these motions. Second, it must resist external forces during flight to prevent unintended arm movements. These performance requirements are derived from simulations of the arm's dynamics under various scenarios, including vertical lift and hover. Furthermore, the folding and deployment mechanism must be designed to accommodate specific design constraints related to the UAM context. For example, the system must reconcile the competing requirements of weight reduction and structural robustness. An increase in the vehicle's weight will inevitably lead to an increase in the energy required for flight, which will in turn result in a reduction in the vehicle's efficiency and range. Conversely, inadequate structural integrity may result in mechanical failure, particularly during high-stress scenarios such as emergency maneuvers or extreme weather conditions.

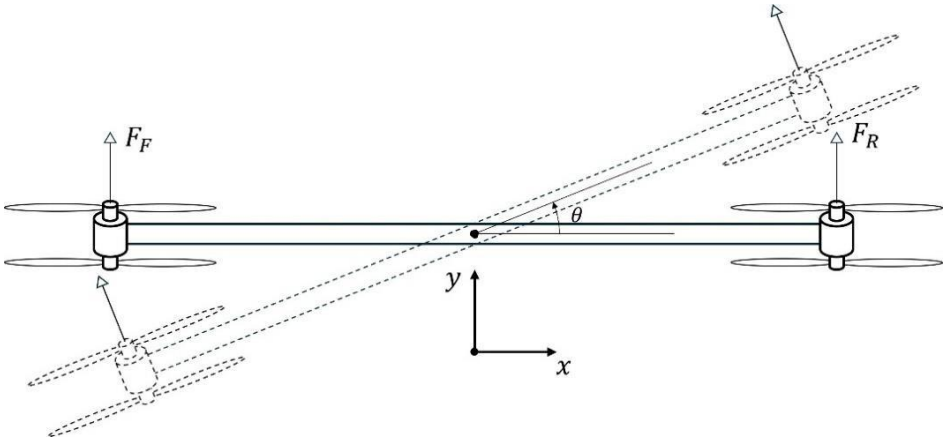

Figure 2: Thrust force distribution during transition.

The following sections present a detailed account of the multibody modeling methodology, the force analysis conducted for the actuator, and the results of these analysis. These findings will inform the selection of an appropriate actuator and provide recommendations for enhancing the mechanism's performance and safety. The incorporation of these findings into the larger context of UAM vehicle design underscores the value of interdisciplinary strategies in addressing the complexities of this evolving field.

3. Multibody modeling methodology

Multibody dynamics offers a robust framework for modeling and analyzing the motion of interconnected mechanical components subjected to forces and constraints. In the context of the folding and deployment mechanism of the flying car's arm, multibody modeling allows the assessment of both dynamic and static performance across a range of operational scenarios. This methodology guarantees a precise representation of the system's kinematics and dynamics, thus offering crucial insights into its behavior.

The fundamental basis of multibody kinematics involves describing the position of a point $\mathbf{r}$ in a moving body relative to a global reference frame. This is expressed by the equation [16, 17]:

$$\mathbf{r} = \mathbf{R} + \mathbf{A}\bar{\mathbf{u}} \tag{1}$$

where $\mathbf{R}$ is the global position vector of the origin of the body reference, $\mathbf{A}$ is the transformation matrix from the body coordinate system to the global coordinate system, and $\bar{\mathbf{u}}$ is the position vector of the arbitrary point with respect to the body coordinate system. This relationship serves as the foundation for deriving velocities and accelerations. The velocity $\dot{\mathbf{r}}$ of the point is obtained by differentiating the position vector with respect to time [16]:

$$\dot{\mathbf{r}} = \dot{\mathbf{R}} + \dot{\mathbf{A}}\bar{\mathbf{u}} = \dot{\mathbf{R}} + \boldsymbol{\omega} \times \mathbf{u} \tag{2}$$

where $\boldsymbol{\omega}$ is the angular velocity vector defined in the global coordinate system. In a similar manner, one can express the absolute acceleration of a given point on a rigid body in terms of generalized orientation coordinates [16, 17].

$$\ddot{\mathbf{r}} = \ddot{\mathbf{R}} + \ddot{\mathbf{A}}\bar{\mathbf{u}} = \ddot{\mathbf{R}} + \boldsymbol{\alpha} \times \mathbf{u} + \boldsymbol{\omega} \times (\boldsymbol{\omega} \times \mathbf{u}) \tag{3}$$

where $\boldsymbol{\alpha}$ is the angular acceleration vector defined in the global coordinate system. Equations (1)-(3) represent the most fundamental equations of the kinematics of MBD. The ability to accurately represent motion is vital for grasping the kinematic behavior of the folding arm mechanism, especially when simulating dynamic deployment

and retraction processes. Furthermore, multibody dynamics introduces equations of motion that govern how the system responds to external forces and moments. Employing the fundamental principles of classical mechanics in conjunction with the mathematical technique of analytical dynamics, which is based on the introduction of Lagrange multipliers, results in the differential-algebraic equations of motion of the multibody system under study assuming the following final form represented in configuration space [18-20]:

$$\begin{cases} \mathbf{M}\ddot{\mathbf{q}} = \mathbf{Q_e} + \mathbf{Q_v} - \mathbf{C_q^T}\boldsymbol{\lambda} \\ \boldsymbol{C} = \mathbf{0} \end{cases} \tag{4}$$

where **M** denotes the system's mass matrix, $\mathbf{Q_v}$ is the quadratic velocity vector capturing system inertia, $\mathbf{Q_v}$ represents the generalized external force vector, and $\mathbf{C_q} = \partial \mathbf{C}/\partial \mathbf{q}$ is the constraint Jacobian matrix derived from the total constraint vector **C**, which encapsulates all kinematic joint constraints, and the vector $\boldsymbol{\lambda}$ contains the Lagrange multipliers associated with these constraints. The system equations of motion given by Equation (4) represent a set of index-3 differential algebraic equations, which can be mathematically transformed in the following equivalent form [21, 22]:

$$\begin{bmatrix} \mathbf{M} & \mathbf{C_q^T} \\ \mathbf{C_q} & \mathbf{0} \end{bmatrix} \begin{bmatrix} \ddot{\mathbf{q}} \\ \boldsymbol{\lambda} \end{bmatrix} = \begin{bmatrix} \mathbf{Q_v} + \mathbf{Q_v} \\ \mathbf{Q_d} \end{bmatrix} \tag{5}$$

where $\mathbf{Q_d}$ represents the system's quadratic velocity vector for constraints. Equation (5) represents a set of index-1 differential-algebraic equations of motion, containing only the independent subset of kinematic constraints meaningful for the dynamic analysis

The vector of generalized coordinates **q** can be obtained as:

$$\boldsymbol{q} = \begin{bmatrix} \boldsymbol{q_1^T} & \boldsymbol{q_2^T} & \cdots & \boldsymbol{q_{N_b}^T} \end{bmatrix}^T \tag{6}$$

where:

$$\boldsymbol{q_i} = \begin{bmatrix} \mathbf{R}_i \\ \boldsymbol{\theta_i} \end{bmatrix}, i = 1, 2, \ldots, N_b \tag{7}$$

In Equation (7) $\boldsymbol{R_i}$ represents the translational coordinates, $\boldsymbol{\theta_i}$ represents the rotational coordinates, and N_b is the number of bodies.

This mathematical formulation provides the basis for the analysis of both the dynamic processes of arm folding and deployment and the static equilibrium of the arm when subjected to flight loads. By solving these equations numerically, it is possible to simulate real-world scenarios and assess the forces and moments acting on the electric actuator and other components. To conduct these analyses, we employ SimScape Multibody, a robust multibody modeling environment integrated with MATLAB. The comprehensive suite of tools provided by SimScape Multibody—which includes the ability to define, simulate, and analyze mechanical systems—makes it an ideal platform for this study. The software's intuitive block diagram interface enables the representation of complex mechanical systems using predefined components, including rigid bodies, joints, and actuators. Figure 3 depicts a block diagram of the aforementioned configuration, elucidating the interrelationship between the mechanical components.

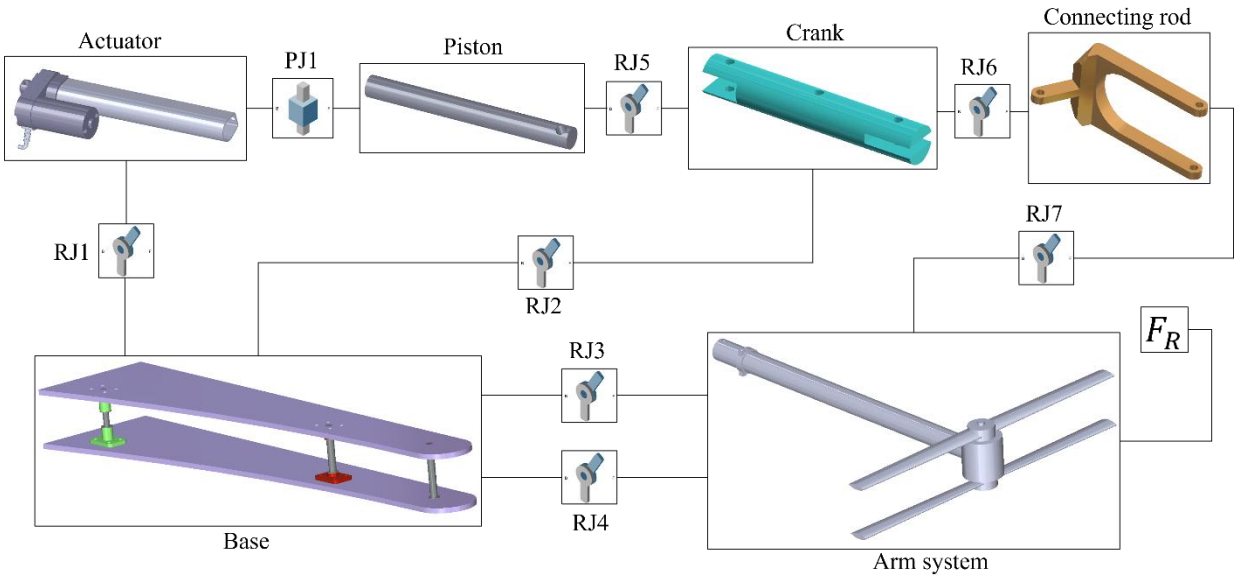

Figure 3: Block diagram of the folding arm mechanism in SimScape Multibody.

The data for the bodies, including the masses and the inertial properties are given in Table 3. The local reference frame for each body is located at the center of mass and oriented such that the orientation of the axes is defined to be aligned with the principal inertia directions of each body.

Table 3: Foldable flying car model body data.

Body	**Mass** (kg)	**Inertia** (kg·m^2) (I_{xx}, I_{yy}, I_{zz})
Base	3.21	0.0095, 0.144, 0.145
Piston	0.07	0.0002, 0.001, 0.001
Actuator	0.49	0.0003, 0.002, 0.002
Crank	0.77	0.0002, 0.003, 0.003
Connecting rod	0.42	0.0005, 0.001, 0.001
Arm system	33.16	0.01, 0.27, 0.28

In this regard, Table 4 presents the spatial information related to the center of mass and orientation of each individual component comprising the propeller folding mechanism. The provided data encompasses both translational and rotational components, articulated within the absolute coordinate system, which is defined by the axes x, y, z. This global reference frame serves as the primary framework throughout the analysis and enables the accurate delineation of the spatial configuration of each body. Consequently, it facilitates a consistent and precise localization of the center of mass and its respective orientation for all components within the multibody system. Conversely, Table 5 presents the localization data for the kinematic joints associated with the different components. The information reported includes the translational and rotational coordinates necessary to position each joint in space. However, it is important to emphasize that both the translational and rotational coordinates in Table 5 are expressed in the local body reference frame of each component. This body-fixed coordinate system, denoted by the axes $\bar{x}, \bar{y}, \bar{z}$, is the same as the one established in Table 4, ensuring consistency in how each component's geometry is referenced. Moreover, the rotational orientation of each joint is described using Euler angles ϕ, ϑ, ψ following the XYZ rotation sequence.

Table 4. Location of the center of mass for the different components in the absolute coordinate system.

Component	**Translational** (x, y, z) (m)	**Rotational** (ϕ, θ, ψ) (rad)
Base	0.2496, -0.01364, 0	0, 0, 0
Actuator	0.0858, 0.02134, 4.431e-5	0, 0, 0
Piston	0.2281, -1.924e-7, -1.981e-4	0, 1.571, 0
Crank	0.5823, 0.079, -3.109e-4	0, 0, 0
Connecting Rod	0.4134, 0.0174, -3.0554e-4	0, 0, 0
Arm system	1.078, 0.1124, -3.104e-4	0, 0, 0

Table 5. Location of the different joints in the body reference system.

Component	**Joint**	**Translational** ($\bar{x}, \bar{y}, \bar{z}$) (m)	**Rotational** ($\bar{\phi}, \bar{\theta}, \bar{\psi}$) (rad)
Base	RJ1	-0.249, 0.013, 0	0, 0, 0
	RJ2	0.163, 0.031, 0	0, 0, 0
	RJ3	0.353, 0.045, 0.027	0, 0, 0
	RJ4	0.353, 0.045, -0.029	0, 0, 0
Actuator	RJ1	-0.085, -0.021, 0	0, 0, 0
	PJ1	0.221, -0.021, 0	0, 1.571, 0
Piston	PJ1	1.075e-4, 0, 0.078	0, 0, 0
	RJ5	1.075e-4, 0, 0.078	0, -1.571, 0
Crank	RJ2	-0.001, -1.797e-4, 3.0554e-4	0, 0, 0
	RJ5	-0.106, -0.017, 0	0, 0, 0
	RJ6	0.092, 0.015, 0	0, 0, 0
Connecting Rod	RJ6	-0.076, -0.046, 0	0, 0, 0
	RJ7	0.1104, -0.011, 0	0, 0, 0
Arm	RJ3	-0.475, -0.081, 0.028	0, 0, 0
	RJ4	-0.475, -0.081, -0.029	0, 0, 0
	RJ7	-0.386, -0.044, -0.045	0, 0, 0

In order to facilitate the dynamic case of folding and deployment, a fifth-degree polynomial trajectory was implemented in order to govern the displacement of the actuator. This trajectory defines the position of the arm as it transitions from a fully deployed state (0 mm) to a fully folded state (180 mm). The selection of a fifth-degree polynomial is of paramount importance, as it guarantees seamless transitions in motion. In particular, this trajectory ensures that both velocity and acceleration are zero at the beginning and end of the motion. This characteristic is essential to prevent abrupt changes in speed or forces, which could result in mechanical stress, vibrations, or instability in the folding mechanism. By ensuring the continuity and smoothness of velocity and acceleration profiles, the fifth-degree polynomial minimizes wear on the components and optimizes the efficiency of the folding process. The aforementioned law is expressed mathematically as follows:

$$x(t) = a_0 + a_1 t + a_2 t^2 + a_3 t^3 + a_4 t^4 + a_5 t^5 \quad (8)$$

In this context, $x(t)$ is the actuator's position at time t, and the coefficients $a_0, a_1, ..., a_5$ are determined to satisfy boundary conditions. These boundary conditions encompass the initial and final positions, as well as the requirement for zero velocity and acceleration at the commencement (t = 0) and conclusion (t = T) of the motion.

4. Results and discussion

The performance of the folding mechanism under both dynamic and static conditions has been evaluated in order to determine the actuator's force requirements and to inform the selection process. This section will present and discuss the findings of these analyses, with a particular focus on the forces generated during the folding and deployment processes, as well as the forces necessary to maintain the mechanism in a deployed state across a range of flight conditions. In the multibody model, a set of generalized coordinates was used, as shown in Equation (5).

4.1. Dynamic analysis: Folding and Deployment

The actuator's displacement was modeled using a fifth-degree polynomial trajectory, with three distinct time points T, to simulate the folding and deployment processes. The times were 10, 20, and 30 seconds. Since the actuator´s motion has been imposed, the inverse dynamic can be used to obtain the value of the actuator force, which is associated with Lagrange multipliers term. By so, Equation (4) leads to:

$$\begin{bmatrix} \ddot{\mathbf{q}} \\ \boldsymbol{\lambda} \end{bmatrix} = \begin{bmatrix} \mathbf{M} & \mathbf{C_q^T} \\ \mathbf{C_q} & \mathbf{0} \end{bmatrix}^{-1} \begin{bmatrix} \mathbf{Q_v} + \mathbf{Q_v} \\ \mathbf{Q_d} \end{bmatrix} \quad (9)$$

which can be solved recursively for each timestep. The impact of the actuation time on the force exerted by the actuator was investigated, and the findings are illustrated in Figure 4.

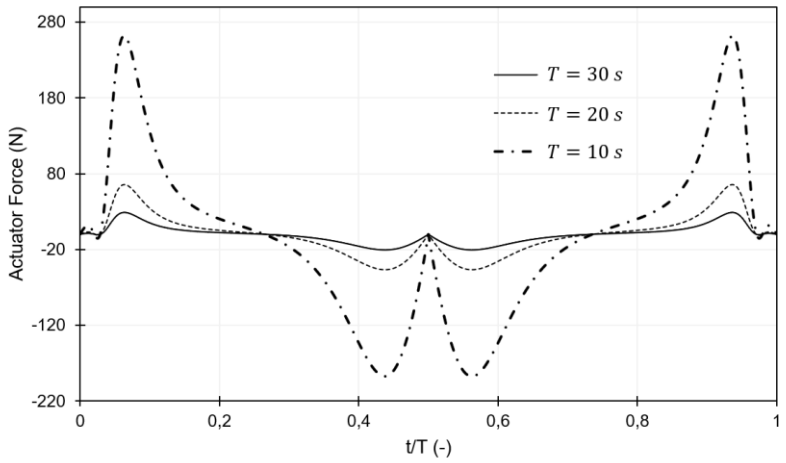

Figure 4: Force profile of the actuator during folding and deployment for different actuation times.

The force required by the actuator demonstrates an inverse relationship with the actuation time. A reduction in time results in an increase in acceleration due to the higher velocity gradients dictated by the shorter interval, which in turn gives rise to greater inertial forces. For a time period of 10 seconds, the maximum force required was 261.8 N. For a time period of 20 seconds, the maximum force decreased significantly to 65.5 N, while for a time period of 30 seconds, the maximum force was 29.1 N. These results highlight the importance of selecting an appropriate actuation time to achieve an optimal balance between performance and energy efficiency, particularly in dynamic scenarios. Furthermore, Figure 5 depicts the motion of the folding arm at pivotal stages throughout the folding procedure. The mechanism undergoes a transition from a fully deployed position (x=0mm) to a semi- folded position (x=90mm) and subsequently to a fully folded position (x=180mm). These positions serve to illustrate the spatial configuration of the arm at different stages of deployment.

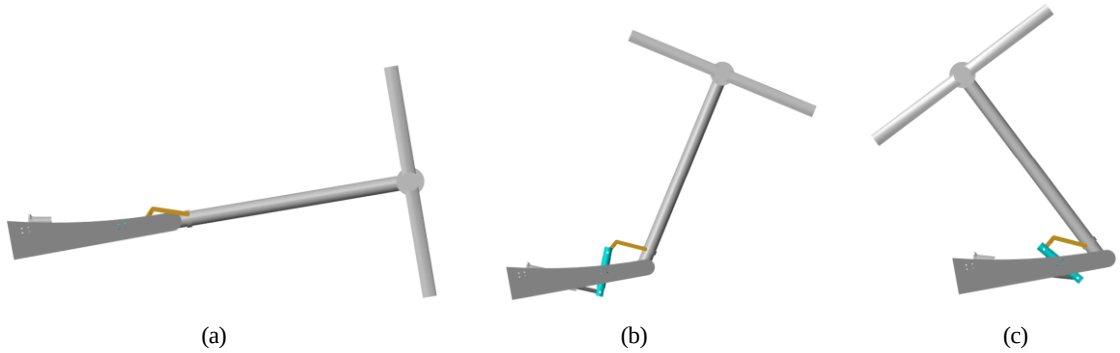

(a) (b) (c)

Figure 5: Positions of the folding mechanism: (a) Fully deployed (x = 0mm), (b) Semi-folded (x = 90mm), and (c) Fully folded (x = 180mm).

4.2. Static analysis: Forces in flight

The analysis also included the force required to maintain the mechanism in a fully deployed state in response to varying flight conditions. The force in question is subject to the influence of the loads acting on the arm as the vehicle operates in both vertical and horizontal flight modes. Figure 6 illustrates the variation in this force as a function of the vehicle's inclination angle θ, which ranges from 0º (vertical flight) to 45º (the maximum safe tilt angle for forward flight). The findings indicate a nearly linear increase in the force demanded by the actuator in conjunction with the inclination angle. At an inclination angle of 45º, the force reaches its maximum value of 1286.3 N. This value represents the maximum aerodynamic load condition, thereby underscoring the critical role of the actuator in stabilizing the mechanism during aggressive flight maneuvers.

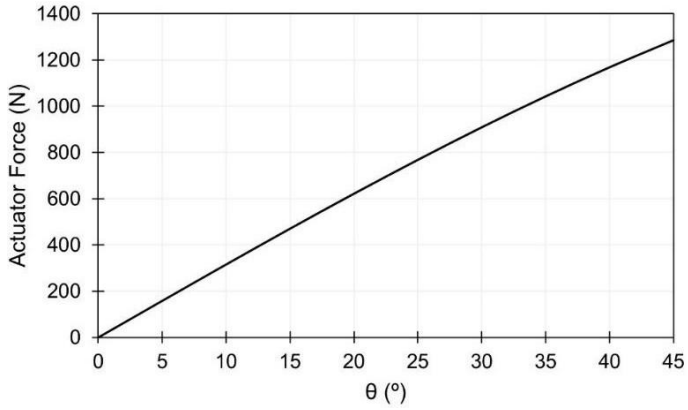

Figure 6: Variation of the force required by the actuator to maintain the mechanism in a deployed state as a function of the vehicle's inclination angle.

The selection of the actuator is driven by the highest force requirement observed, based on the analysis of folding and deployment as well as static forces during flight. The dynamic analysis revealed a peak force of 261.8 N for the shortest actuation time, whereas the static analysis under flight conditions demonstrated a significantly higher force requirement of 1286.3 N at θ = 45º. Therefore, the actuator must be capable of generating a force of at least 1286.3 N to ensure safe operation under the most demanding conditions. In addition to the aforementioned force requirement, the actuator must also accommodate a displacement of 180 mm, which corresponds to the full range of motion of the folding arm. The dual requirement of high force and adequate displacement thus defines the specifications for the actuator, which must be selected in a manner that ensures reliability and robustness.

5. Summary, conclusions and research perspectives

The objective of this study was to conduct a mechanical analysis of a folding arm mechanism for a flying car, with the aim of determining the force requirements of the electric actuator during both dynamic and static conditions. The analysis was conducted using a multibody model developed in SimScape Multibody within MATLAB. Two specific scenarios were subjected to evaluation: the dynamic folding and deployment of the arm, and the static forces experienced during various flight conditions. The results of the dynamic analysis demonstrated a discernible correlation between actuation time and force demand. The results demonstrated that shorter actuation times led to a notable increase in the force required by the actuator, underscoring the necessity for meticulous timing selection to achieve an optimal balance between mechanical performance and efficiency. For example, the maximum force for a deployment time of 10 seconds was 261.8 N, while for a longer time of 30 seconds, the force was reduced to 29.1 N. The static analysis considered the aerodynamic forces acting on the arm under different flight inclinations,

from vertical (θ = 0º) to a maximum tilt of 45º.

The results demonstrated a nearly linear increase in the force necessary to maintain the arm in a deployed position, with a peak force of 1286.3 N at an angle of 45 degrees. This condition represents the most challenging scenario for the actuator, underscoring its vital function in ensuring stability during flight. The results indicate that the actuator must satisfy two fundamental design criteria. First and foremost, the actuator must be capable of generating a maximum force of 1286.3 N, as is required under static flight conditions. Secondly, the actuator must be capable of accommodating a displacement of 180 mm in order to facilitate the complete folding and deployment of the arm. These specifications are fundamental to guarantee the secure and effective operation of the folding mechanism. Moreover, the implementation of a fifth-degree polynomial trajectory for dynamic motion ensured the attainment of seamless transitions with zero velocity and acceleration at the commencement and conclusion of the operational cycle. This approach serves to minimize stress on the components, thereby reducing wear and extending the operational life of the mechanism.

This work establishes a foundation for future research in several pivotal areas. The optimization of the material could result in a reduction of the overall weight of the mechanism while maintaining its structural integrity. The development of advanced control algorithms, such as predictive or adaptive control, has the potential to further enhance actuator performance under varying conditions. The incorporation of detailed aerodynamic models into the simulation would enhance the precision of force predictions, particularly in the context of complex flight maneuvers. The experimental validation of these simulation results is a crucial subsequent step, as it would confirm the reliability of the findings and address any discrepancies between the theoretical models and real-world behavior. Ultimately, future studies should investigate the integration of the folding arm into the complete vehicle system, ensuring compatibility and robustness under operational conditions. This study offers invaluable insights into the design and operation of folding mechanisms for urban air mobility, thereby contributing to the advancement of safe and efficient flying car systems.

6. References

[1] A. Bauranov, J. Rakas, Designing airspace for urban air mobility: A review of concepts and approaches, Progress in Aerospace Sciences 125 (2021) 100726. doi: https://doi.org/10.1016/j.paerosci.2021.100726.

[2] A. Straubinger, R. Rothfeld, M. Shamiyeh, K.-D. Büchter, J. Kaiser, K. O. Plötner, An overview of current research and developments in urban air mobility – setting the scene for uam introduction, Journal of Air Transport Management 87 (2020) 101852. doi: https://doi.org/10.1016/j.jairtraman.2020.101852.

[3] O. A. Marzouk, Urban air mobility and flying cars: Overview, examples, prospects, drawbacks, and solutions, Open Engineering 12 (2022) 662–679. doi: https://doi.org/10.1515/eng-2022-0379.

[4] C. Choudhary, Aastha, G. K. Saini, Kunal, M. Saxena, Evaluation of potential flying cars, in: 2023 2nd International Conference for Innovation in Technology (INOCON), 2023, pp. 1–5. doi: https://doi.org/10.1109/INOCON57975.2023.10101276.

[5] S. Mintchev, L. Daler, G. L'Eplattenier, L. Saint-Raymond, D. Floreano, Foldable and self-deployable pocket sized quadrotor, in: 2015 IEEE International Conference on Robotics and Automation (ICRA), 2015, pp. 2190–2195. doi: https://doi.org/10.1109/ICRA.2015.7139488.

[6] M. A. Fenelon, T. Furukawa, Design of an active flapping wing mechanism and a micro aerial vehicle using a rotary actuator, Mechanism and Machine Theory 45 (2010) 137–146. doi: https://doi.org/10.1016/j.mechmachtheory.2009.01.007.

[7] W. Hu, Z. Yang, Y. Gu, Aeroelastic study for folding wing during the morphing process, Journal of Sound and Vibration 365 (2016) 216–229. doi: https://doi.org/10.1016/j.jsv. 2015.11.043.

[8] I. Wang, E. H. Dowell, Structural dynamics model of multisegmented folding wings: Theory and experiment, Journal of Aircraft 48 (2011) 2149–2160. doi: https://doi.org/10.2514/1.C031509.

[9] R. L. Huston, Multibody dynamics — modeling and analysis methods, Applied Mechanics Reviews 44 (1991) 109–117. doi: https://doi.org/10.1115/1.3119496.

[10] F. Amirouche, Fundamentals of multibody dynamics: theory and applications, Springer Science & Business Media, 2007

[11] Y. Huang, X. Guo, D. Cao, Aerodynamic characteristics of a z-shaped folding wing, Aerospace 10 (2023). doi: https://doi.org/10.3390/aerospace10090749

[12] D. Tang, E. H. Dowell, Theoretical and experimental aeroelastic study for folding wing structures, Journal of Aircraft 45 (2008) 1136–1147. doi: https://doi.org/10.2514/1.32754.

[13] H. Xu, J. Han, H. Yun, X. Chen, Calculation of the hinge moments of a folding wing aircraft during the flight-folding process, International Journal of Aerospace Engineering 2019 (2019) 9362629. doi: https://doi.org/10.1155/2019/9362629.

[14] B. Obradovic, K. Subbarao, Modeling of flight dynamics of morphing wing aircraft, Journal of Aircraft 48 (2011) 391–402. doi: https://doi.org/10.2514/1.C000269.

[15] C. Pérez-Carrera, O. E. Genel, R. La Regina, C. M. Pappalardo, D. Guida, A comprehensive and systematic literature review on flying cars in contemporary research, Journal of Applied and Computational Mechanics (2024). doi: https://doi.org/10.22055/jacm.2024.47083.4658.

[16] C. M. Pappalardo, T. Magaldi, L. Masucci, R. La Regina, A. Naddeo, Virtual prototyping, multibody dynamics, and control design of an adaptive lift table for material handling, Journal of Applied and Computational Mechanics 10 (2024) 659–693. doi: https://doi.org/10.22055/jacm.2024.45269.4342.

[17] Russell, K., Shen, J.Q., & Sodhi, R. (2022). Kinematics and Dynamics of Mechanical Systems: Implementation in MATLAB® and Simscape Multibody™ (3rd ed.). CRC Press. https://doi.org/10.1201/9781003316961.

[18] C. M. Pappalardo, R. La Regina, D. Guida, Multibody modeling and nonlinear control of a pantograph scissor lift mechanism, Journal of Applied and Computational Mechanics 9 (2023) 129–167. doi: https://doi.org/10.22055/jac m.2022.40537.3605.

[19] C. A. Manrique-Escobar, C. M. Pappalardo, and D. Guida, On the Analytical and Computational Methodologies for Modelling Two-wheeled Vehicles within the Multibody Dynamics Framework: A Systematic Literature Review, *Journal of Applied and Computational Mechanics*, vol. 8, no. 1, pp. 153–181 (2022). doi: https://doi.org/10.22055/jacm.2021.37935.3118

[20] C. A. Manrique-Escobar, C. M. Pappalardo, D. Guida, A Multibody System Approach for the Systematic Development of a Closed-Chain Kinematic Model for Two-Wheeled Vehicles. *Machines* (2021), *9*, 245. https://doi.org/10.3390/machines9110245

[21] C. M. Pappalardo, D. Guida, A comparative study of the principal methods for the analytical formulation and the numerical solution of the equations of motion of rigid multibody systems. *Arch Appl Mech* 88, 2153–2177 (2018). https://doi.org/10.1007/s00419-018-1441-3

[22] Miller, S., Soares, T., Weddingen, Y., & Wendlandt, J. (2017). Modeling flexible bodies with simscape multibody software. *An Overview of Two Methods for Capturing the Effects of Small Elastic Deformations*.